Preparation of ethylene/α-olefins copolymers using $(2\text{-RInd})_2ZrCl_2$/MCM-41 (R:Ph,H) catalyst, microstructural study

Saied Ahmadjo, Hassan Arabi, Gholamhossien Zohuri, Mehdi Nekoomanesh, Gholamreza Nejabat & Seyed Mohammad Mahdi Mortazavi

Journal of Thermal Analysis and Calorimetry
An International Forum for Thermal Studies

ISSN 1388-6150
Volume 116
Number 1

J Therm Anal Calorim (2014)
116:417-426
DOI 10.1007/s10973-013-3552-y

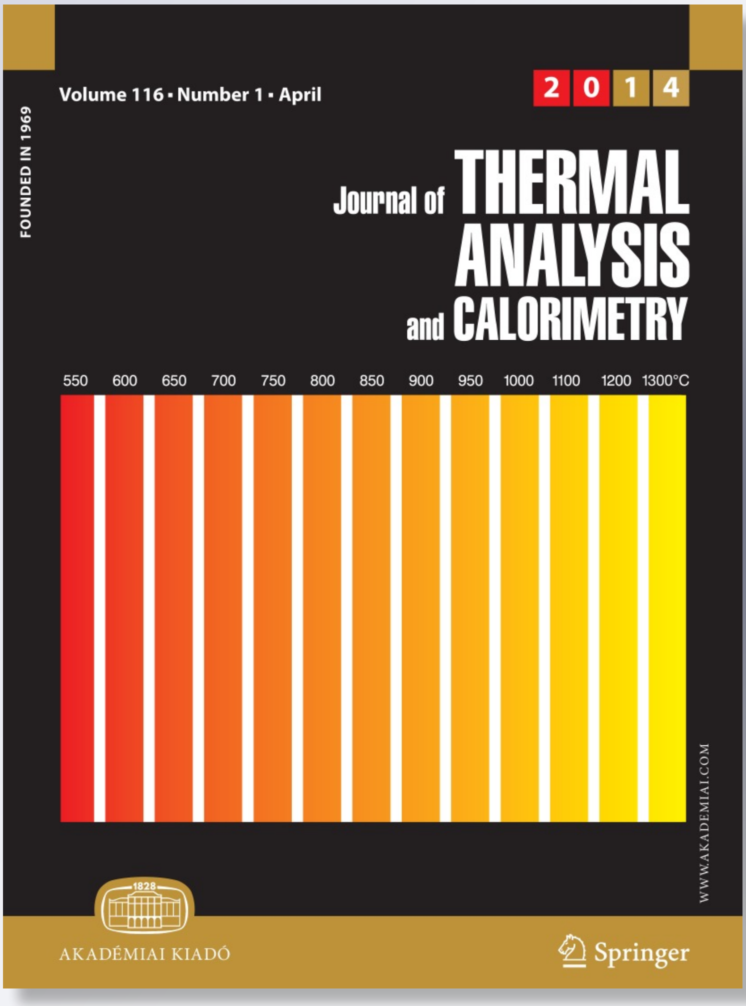

J Therm Anal Calorim (2014) 116:417–426
DOI 10.1007/s10973-013-3552-y

Preparation of ethylene/α-olefins copolymers using (2-RInd)$_2$ZrCl$_2$/MCM-41 (R:Ph,H) catalyst, microstructural study

**Saied Ahmadjo · Hassan Arabi · Gholamhossien Zohuri ·
Mehdi Nekoomanesh · Gholamreza Nejabat ·
Seyed Mohammad Mahdi Mortazavi**

Received: 8 April 2013 / Accepted: 15 November 2013 / Published online: 8 December 2013

Abstract (2-RInd)$_2$ZrCl$_2$ (R:Ph,H) catalyst was supported on MCM-41 and ethylene copolymerization behavior as well as microstructure of copolymers were studied. A steady rate–time profile behavior was observed for homo and copolymerization of ethylene using supported catalysts. It was noticed that increasing the comonomer content can result in lower physical properties. The obtained results indicated that (2-PhInd)$_2$ZrCl$_2$/MCM-41 had higher ability of comonomer incorporation than the non-substituted supported catalysts. The CCC, CCE, and ECC (C: comonomer, E: ethylene) triad sequence distribution in backbone of copolymers were negligible, that means no evidence could be detected for comonomer blocks. The polymer characterization revealed that utilizing 1-octene instead of 1-hexene as the comonomer leads to more heterogeneous distribution of chemical composition. The heterogeneity of the chemical composition distribution and the physical properties were influenced by the type of comonomer and catalyst. (2-PhInd)$_2$ZrCl$_2$/MCM-41 produced copolymers containing narrower distribution of lamellae (0.3–1 nm) than the copolymer produce using Ind$_2$ZrCl$_2$/MCM-41 (0.3–1.6 nm).

Keywords Metallocene catalyst · Copolymerization · Copolymer composition distribution · DSC · Crystallinity

Introduction

Polyolefin market is the largest volume polymer trade in the world today [1, 2]. Their production is estimated to reach 165 Mt year^{-1} in 2018 [3]. In this category copolymers of ethylene with 1-alkenes such as propylene, 1-butene, 1-hexene, and 1-octene are very important commercial products [4–6]. This type of polymer has many advantages such as good mechanical properties, low density, and good process ability [4, 7]. There have been many efforts toward finding more efficient catalyst to produce copolymers with desired properties. Conventional Z–N catalysts result in broad molecular mass distribution, heterogeneous chemical composition distribution (CCD), and low comonomer incorporation while metallocene types have shown some indisputable advantages such as good comonomer incorporation and uniform CCD [8–10]. These advantages have brought m-LLDPE a high growth rate comparable to Z–N LLDPE [11].

However, the homogenous form of metallocene has some disadvantages: high consumption of MAO, lack of morphology control, and reactor fouling are the most important ones [12–15]. To overcome these drawbacks, the metallocene catalyst could be anchored on to inorganic carries such as silica, MCM-41, MgCl$_2$, or polymeric supports [16–20]. By using the supported metallocene, the morphology of polymer particles is modified and reactor fouling is reduced and they can be used for new technologies like gas phase process [21, 22].

To be more successful in this filed it was needed to know the properties of m-LLDPE including the average

---

S. Ahmadjo (✉) · H. Arabi · M. Nekoomanesh · G. Nejabat ·
S. M. M. Mortazavi (✉)
Department of Catalyst, Iran Polymer and Petrochemical
Institute, P.O. Box 14965/115, Tehran, Iran
e-mail: s.ahmadjo@ippi.ac.ir

S. M. M. Mortazavi
e-mail: m.mortazavi@ippi.ac.ir

G. Zohuri
Department of Chemistry, Faculty of Science, Ferdowsi
University of Mashhad, P.O. Box 1436, Mashhad, Iran

molecular mass and its distribution, degree of crystallinity and melting temperature, the chemical composition distribution of polymer, comonomer content (composition) which in turn essentially depends on polymerization condition (temperature, Al/Zr, and feed composition) and catalytic system [23]. Thus, the nature of the catalysts (type of ligand in metallocene and presence of supports) has a profound influence on the resulting microstructure of the polymer and therefore on its final properties [24]. To investigate the microstructure of ethylene copolymers several powerful techniques can be used. NMR is the most popular technique which is used to obtain the most precise and reliable information about comonomer content and its distribution through the backbone of polymer [25–27]. GPC is another method that is generally used for monitoring molecular mass and its distribution and finally DSC, TREF, and Crystaf are the other characterization methods that are widely used for identifying chemical composition distribution of the copolymers [28–30].

In continuation of our previous works on microstructural study of ethylene/α-olefins copolymers produced by (2-PhInd)$_2$ZrCl$_2$ homogeneous catalyst [31] a similar study is done on the microstructure of ethylene copolymers that was produced by (2-PhInd)$_2$ZrCl$_2$/MCM-41 heterogeneous catalyst.

Experimental

Materials

Spherical MCM-41 support was synthesized according to Nekoomanesh et al. [32]. Methylaluminoxane (MAO) in toluene (10 mass%) and triisobutylaluminum (TiBA) were supplied from Aldrich. (2-RInd)$_2$ZrCl$_2$ (R:Ph,H) was synthesized according to literature [31, 33]. 1-Hexene and 1-octene were provided from Merck Chemical Co. (Munich, Germany) and all of them were refluxed and distilled over drying agent before use and kept over 4A/13X activated molecular sieves. Ethylene was obtained from Arak Petrochemical Company (Arak, Iran). Toluene and heptane were dried over CaCl$_2$ by distillation. All the manipulation involving air and/or water sensitive compounds were performed under atmosphere of dried N$_2$ in a glove box.

Support treatment

For preparation of MCM-41 pretreated with MAO, 5 g of MCM-41 was calcinated under atmosphere of N$_2$ at 250 °C for 5 h. 1 g of the dehydroxylated MCM-41 was suspended in toluene. Afterward 4 mL of MAO (10 mass% in toluene) was added to the suspension and stirred over night. The obtained MCM-41 was washed using toluene and heptane four times and the final suspension was used as the support in the polymerization.

Copolymerization

Copolymerization of ethylene with 1-hexene and 1-octene were carried out in a 1-L Buchi reactor (Buchiglauster bmd300) equipped with controlling systems of feeding, temperature, stirring speed, and reaction pressure. Heptane was introduced into the reactor (450 mL) and saturated with ethylene (101 kPa pressure) at the reaction temperature. Polymerization components including TiBA, modified support, and the catalyst solutions were added, respectively. Sufficient amount of comonomer was added to the reactor just before introduction of the catalyst itself. For copolymerization of ethylene with 1-hexene the comonomer was introduced at 20 °C following to that the temperature was adjusted to the reaction temperature. At the end of the polymerization (usually 30 min) the content of the reactor was poured into an excess of acidified methanol, filtrated and dried at 60 °C.

Polymer characterization

All the DSC results were obtained using Mettler-Toledo instrument 823^e Model, interfaced to a digital computer equipped with Star E 9.01 software (Sencor FRS5). The sample was heated from room temperature to 160 °C with the rate of 10 °C min^{-1} and remained for 10 min at the temperature; followed by cooling to 0 °C with a cooling rate of -10 °C min^{-1}. Finally, the polymer was reheated to 160 °C using the same heating rate. The melting point (T_m) and crystallinity (X) were determined according to the results obtained in the last heating cycle. The molecular masses and their distributions were determined through high temperature gel permeation chromatography (Waters GPCV 150+), using 1,2,4-trichlorobenzene as the eluent at 140 °C. ^{13}C NMR analyses of the samples were recorded using a BRUKER 400 AVANCE NMR Instrument. The samples were dissolved in a mixture of deuterated *o*-dichlorobenzene and 1,1,2,2-tetrachloroethane at 120 °C. The comonomer composition distribution (CCD) of the copolymers was determined through analytical TREF and stepwise fractionation of samples by DSC.

Results and discussion

Kinetic study

Ethylene copolymers were produced using 1-hexene and 1-octene in feed. The rate/time profiles of copolymerization

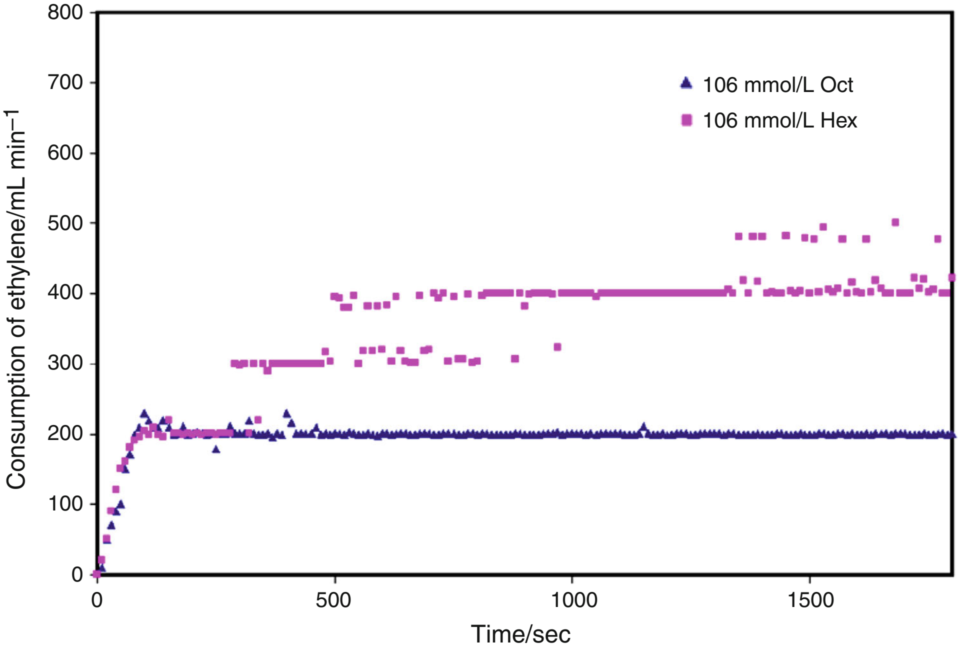

Fig. 1 Profile of rate versus time for copolymerization of ethylene/α-olefin, conditions: temp. = 60 °C, monomer pressure = 600 kPa, [Al]/[Zr] = 70:1, heptane = 450 mL, [Cat] = 1.0×10^{-5} mol Zr

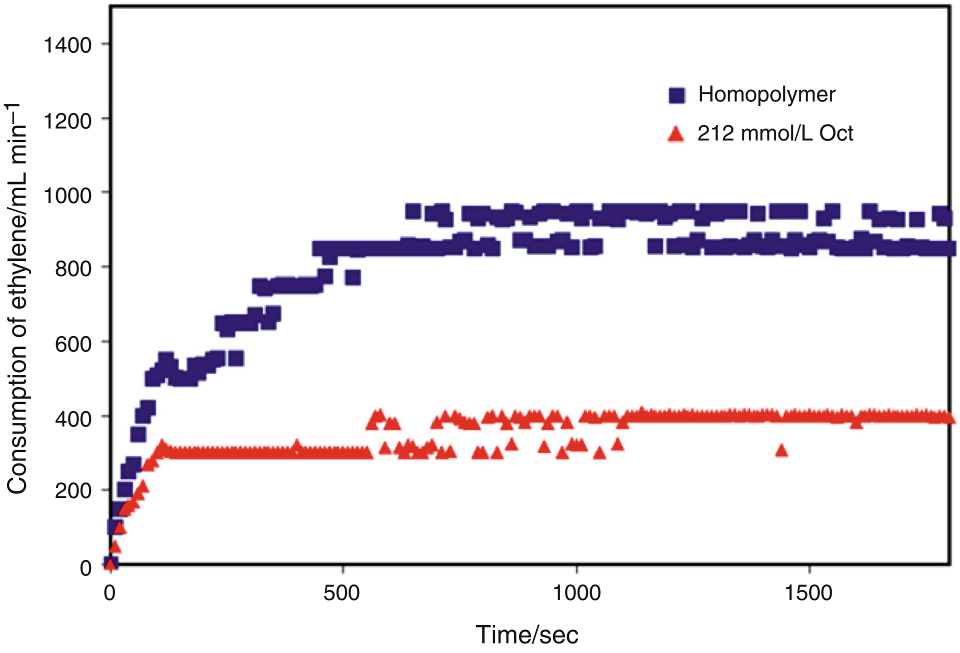

Fig. 2 Comparison of profile of rate versus time for homopolymerization and copolymeriztion of ethylene/1-octene, conditions: temp. = 60 °C, monomer pressure = 600 kPa, [Al]/[Zr] = 70:1, heptane = 450 mL, [Cat] = 1.0×10^{-5} mol Zr

are shown in Figs. 1, 2, and 3. The term "comonomer effect factor" (CEF) and decay index (DI) are defined as Rp_{av}(co)/Rp_{av}(homo) and $Rp_{(max)}/Rp_{(min)}$ (Rp_{av} is the average rate of polymerization, $Rp_{(max)}$ is the maximum rate of polymerization, and $Rp_{(min)}$ is the rate of polymerization at 30 min), respectively, which were used to follow the kinetic behavior of the catalyst. The kinetic results are listed in Table 1. The observed results of CEF < 1 indicates that a depression effect happened on the CEF for polymerization of the supported catalyst with increasing the monomer concentration and molar mass of comonomer in feed. The descending trend observed for CEF in copolymerization may be attributed to a competitive coordination of the comonomer to the active center resulting in a possible deactivation of some catalytic centers [33, 34]. According to Table 1 and Figs. 1, 2, 3 it was clearly observed that for the supported catalyst, DI values decreased relative to homogenous form and approached to one. This reduction in catalyst deactivation was attributed to the stability of active center by immobilization of catalyst and reduction of bimolecular process [35, 36].

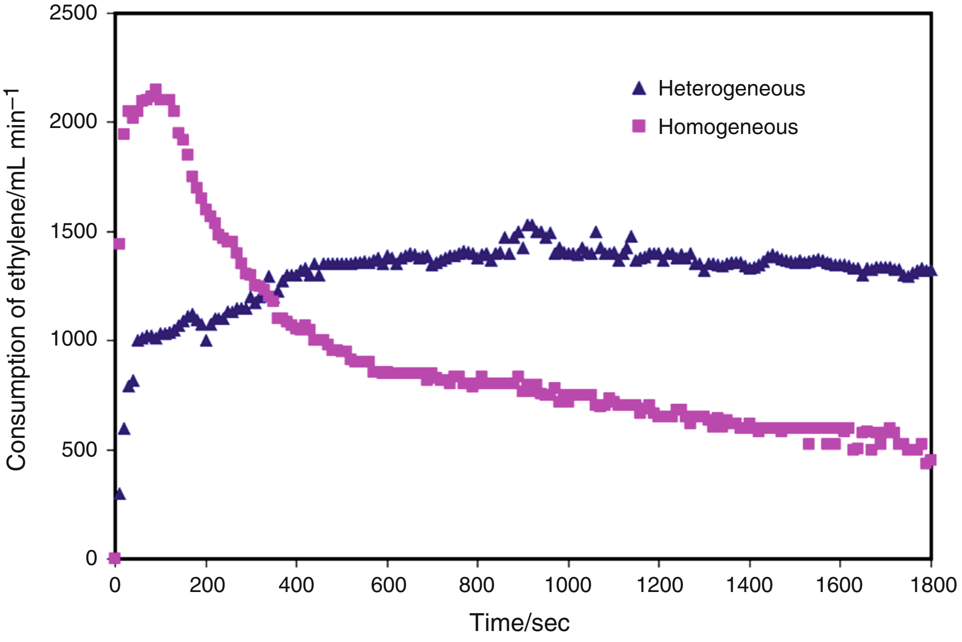

Fig. 3 Comparison profile of rate versus time for homopolymerization of ethylene using supported and non-supported Ind_2ZrCl_2 catalyst

Table 1 Kinetic parameters of ethylene copolymerization

Comonomer concentration/ mmol L^{-1}		Activity ($\times 10^{-3}$)/ g PE (mmol Zr h)$^{-1}$	CEF	Decay index
0		11.3	1.00	1.0
106	Hex	5.6	0.49	1.0
	Oct	4.5	0.40	1.0
212	Hex	5.2	0.46	1.0
	Oct	2.4	0.21	1.0
	Oct	0.7	–	–

Conditions: temp = 60 °C, monomer pressure = 606 kPa, $[Al]_{MAO}/[Zr] = 70{:}1$, [TiBA] = 2 mmol, toluene = 450 mL, $[Ind_2ZrCl_2] = 1.0 \times 10^{-5}$ mol Zr, MCM-41 = 100 mg

Study of properties and microstructure of ethylene copolymers

Table 2 shows the physical properties of ethylene/1-hexene and ethylene/1-octene copolymers. They include melting temperature (T_m), crystallinity (X), molecular mass, molecular mass distribution (MWD), and number of branch per 1,000 carbon of backbone chain. As can be seen from the table, as the comonomer content in feed increased, melting temperature, crystallinity, and molecular mass of the copolymer decreased. By increasing the comonomer concentration in polymerization medium and by decreasing the molecular mass of the used comonomer, which may result in more chain transfer reactions through β-hydride

Table 2 Physical properties of ethylene copolymers

Comonomer concentration/ mmol L^{-1}	% mol comonomer in polymer	T_m/ °C	X/%	M_n	M_w	PDI	nb/ 1000C	CCC	EEC + CEE	CEC	ECE	ECC + CCE	EEE
Ind_2ZrCl_2/MCM-41 (ethylene/1-hexene)													
106	0.8	129.2	33.4	106,382	689,248	6.5	4.8	0.35	1.24	0.00	0.16	0.00	98.26
212	1.3	126.5	29.5	83,064	484,357	5.8	6.6	0.61	1.93	0.00	0.82	0.00	96.64
$(2\text{-PhInd})_2ZrCl_2$/MCM-41(ethylene/1-hexene)													
106	2.2	117.4	14.5	163,453	1,297,642	7.9	13.7	1.54	3.51	0.00	2.01	0.49	94.00
212	5.4	114.2	–	155,599	992,939	6.4	32.0	0.00	7.95	0.00	4.20	0.00	86.31
Ind_2ZrCl_2/MCM-41 (ethylene/1-octene)													
106	0.7	133.0	38.3	140,371	1,027,411	7.3	4.5	0.00	0.78	0.00	0.30	0.00	98.91
212	1.1	129.6	34.3	113,283	784,268	6.9	5.4	0.00	1.38	0.00	0.75	0.00	97.88
$(2\text{-PhInd})_2ZrCl_2$/MCM-41 (ethylene/1-octene)													
106	2.1	–	–	–	–	–	10.8	0.00	2.56	0.00	1.47	0.00	95.97
212	3.7	115.7	15.4	142,636	1,318,415	9.2	21.1	0.00	5.70	0.00	2.75	0.00	91.55

X crystallinity, *PDI* polydispersity index

Table 3 Lamellar thickness and DI value of ethylene/1-octene copolymer and its distribution ($(Ind)_2ZrCl_2$/MCM-41)

1-Octene concentration/ mmol L^{-1}	Peak no.	T_m/°C	l_c/nm	Mass/%	DSCI
106	1	131.2	1.96	45.0	1.00
	2	125.8	1.28	32.3	0.72
	3	117.5	0.84	9.3	0.21
	4	107.8	0.6	8.9	0.20
	5	101.2	0.5	0.1	0.01
	6	97.0	0.45	1.4	0.01
	7	91.1	0.4	0.6	0.01
	8	86.1	0.36	2.4	0.05
212	1	128.8	1.59	51.4	1.00
	2	122.0	1.03	26.6	0.52
	3	114.8	0.75	7.1	0.14
	4	108.6	0.61	5.4	0.10
	5	102.5	0.52	3.4	0.07
	6	96.4	0.45	2.5	0.05
	7	90.5	0.4	1.8	0.03
	8	84.7	0.35	1.2	0.02
	9	78.8	0.32	0.6	0.01

Table 4 Lamellar thickness and DI value of ethylene/1-hexene copolymer and its distribution ($(Ind)_2ZrCl_2$/MCM-41)

1-Hexene concentration/ mmol L^{-1}	Peak no.	T_m/°C	l_c/nm	Mass/%	DSCI
106	1	129.0	1.61	54.4	1.00
	2	122.1	1.04	25.2	0.46
	3	114.8	0.75	6.8	0.13
	4	108.7	0.61	5.2	0.10
	5	102.5	0.52	3.3	0.06
	6	96.6	0.45	2.3	0.04
	7	90.7	0.4	1.4	0.03
	8	84.8	0.36	1.0	0.02
	9	79.2	0.32	0.4	0.01
212	1	127.4	1.43	20.9	0.59
	2	121.9	1.03	35.6	1.00
	3	114.6	0.75	16.0	0.45
	4	108.3	0.61	10.4	0.29
	5	102.1	0.51	5.7	0.16
	6	96.2	0.44	4.9	0.14
	7	90.2	0.39	2.5	0.07
	8	84.5	0.35	2.4	0.07
	9	78.5	0.32	0.9	0.03
	10	73.1	0.29	0.7	0.02

Table 5 Lamellar thickness and DI value of ethylene/1-octene copolymer and its distribution ($(2\text{-}PhInd)_2ZrCl_2$/MCM-41)

1-Octene concentration/ mmol L^{-1}	Peak no.	T_m/°C	l_c/nm	Mass/%	DSCI
106	1	134.2	2.76	2.1	0.09
	2	128.3	1.53	1.0	0.04
	3	121.3	1	11.7	0.50
	4	115.4	0.77	23.2	1.00
	5	109.1	0.62	21.9	0.94
	6	102.9	0.52	15.8	0.68
	7	96.7	0.45	9.7	0.42
	8	90.6	0.4	6.5	0.28
	9	84.6	0.35	4.3	0.19
	10	79.0	0.32	2.1	0.09
	11	73.5	0.3	1.6	0.07
212	1	134.0	2.69	10.8	0.78
	2	128.4	1.54	6.6	0.48
	3	121.1	0.99	9.0	0.65
	4	114.8	0.75	12.0	0.87
	5	108.5	0.61	13.9	1.00
	6	102.4	0.52	12.0	0.87
	7	96.3	0.45	10.8	0.78
	8	90.3	0.39	11.4	0.83
	9	84.4	0.35	9.0	0.65
	10	78.5	0.32	4.2	0.30

elimination or transfer to comonomer [37–39], the comonomer content and therefore the number of branches increased in the resulting copolymers. 1-Hexene as comonomer showed higher activity and higher incorporation into the polymer chains than 1-octene. Higher concentration of comonomer increased the possibility of its incorporation into the polymer chains. Consequently, higher number of branches in the copolymer caused melting temperature and crystallinity of the copolymer to decrease [40–42].

Physical properties and comonomer sequence distribution show that 2-phenyl substitution on indenyl ligand causes the catalyst to incorporate more comonomer into the copolymer chains, which can affect physical properties and comonomer sequence distribution of comonomer through the chains. It was observed that the 2-phenyl type catalyst resulted in higher molecular mass copolymer than non-substituted one which is in complete accordance with steric and electronic effects of substituents of ligands in the catalyst [43].

CCD study of ethylene copolymers using $(2\text{-}RInd)_2ZrCl_2$/MCM-41 (R:Ph,H) catalyst

Study of the effect of catalyst type on heterogeneity of comonomer incorporation is a very important subject which can result in better understanding of copolymer

Table 6 Lamellar thickness and DI value of ethylene/1-hexene copolymer and its distribution ((2-PhInd)$_2$ZrCl$_2$/MCM-41)

1-Hexene concentration/mmol L^{-1}	Peak no.	T_m/°C	l_c/nm	Mass/%	DSCI
106	1	127.1	1.4	0.2	0.01
	2	121.5	1.01	12.4	0.52
	3	115.5	0.77	23.8	1.00
	4	109.3	0.63	23.5	0.99
	5	103.0	0.52	15.8	0.66
	6	96.8	0.45	9.7	0.41
	7	90.7	0.4	6.4	0.27
	8	84.6	0.35	4.4	0.18
	9	78.8	0.32	2.2	0.09
	10	72.7	0.29	1.5	0.06
212	1	121.1	0.99	1.1	0.04
	2	114.8	0.75	4.9	0.19
	3	108.7	0.61	9.3	0.36
	4	102.6	0.52	12.1	0.46
	5	96.6	0.45	17.5	0.67
	6	90.8	0.4	26.2	1.00
	7	84.9	0.36	19.9	0.76
	8	78.9	0.32	9.0	0.34

behavior. The short chain branch distribution (SCBD), also referred as CCD, of copolymers significantly affects the physical and thermal properties of copolymers [44, 45]. It is therefore necessary to have quantitative methods to find the heterogeneity of microstructure of copolymers. The most common technique for this purpose is temperature rising elution fractionation (TREF) which has been used for several years [46–49]. Through the very tedious procedure of TREF, other new and easier techniques such as crystallization analysis fractionation (Crystaf), stepwise DSC were developed and used as common technique in polyolefin characterization [50–53]. In this method during the isothermal crystallization steps, the separation of the crystalline material into groups of lamellae of different thicknesses occurs depending on the amount and distribution of the α-olefin units in the macromolecular chains.

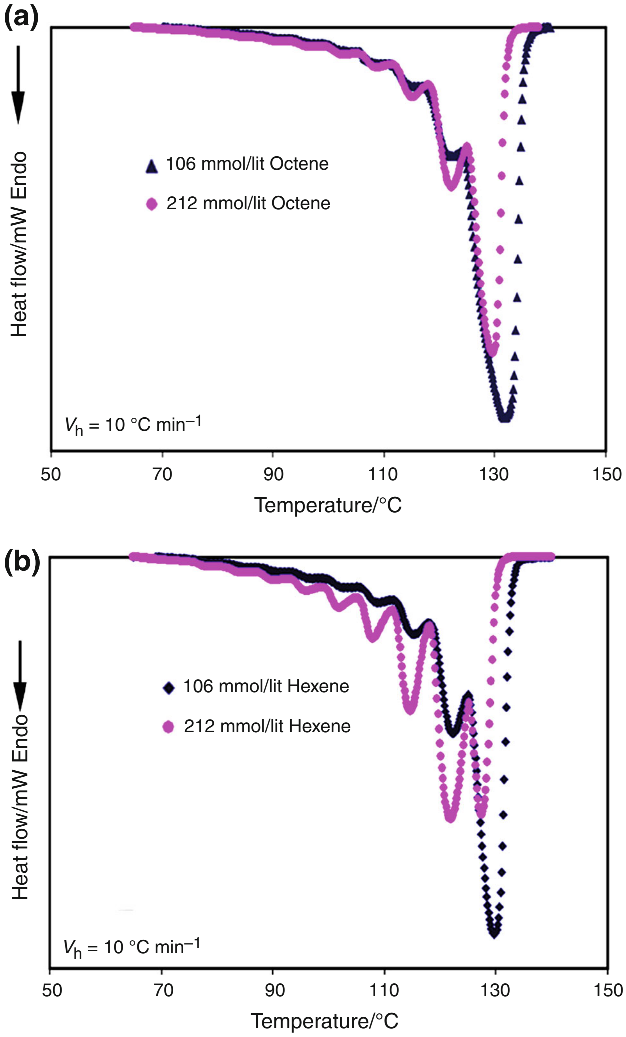

Fig. 4 Effect of 1-octane (**a**) and 1-hexene (**b**) concentrations on the *melting curves* of ethylene copolymers obtained using (Ind)$_2$ZrCl$_2$/MCM-41 catalyst and the SSA method

The DSC curves were deconvoluted to weighted summation of standard Lorentzian distribution functions. The multiplicity of the endotherm peak is related to different lamellar thicknesses of the sample used. For determination of the heterogeneity of the copolymer the DSC index

Table 7 Mass, numerical average, and polydispersity of lamellae thickness distribution

	Ind$_2$ZrCl$_2$/MCM-41				(2-PhInd)$_2$ZrCl$_2$/MCM-41			
	Hexene		Octene		Hexene		Octene	
Comonomer concentration/mmol L^{-1}	106	212	106	212	106	212	106	212
l_n	10.58	7.79	11.71	10.17	5.78	4.26	5.85	5.82
l_m	12.60	9.21	14.45	12.19	6.40	4.50	6.84	8.59
PDI	1.191	1.183	1.234	1.199	1.107	1.057	1.170	1.47

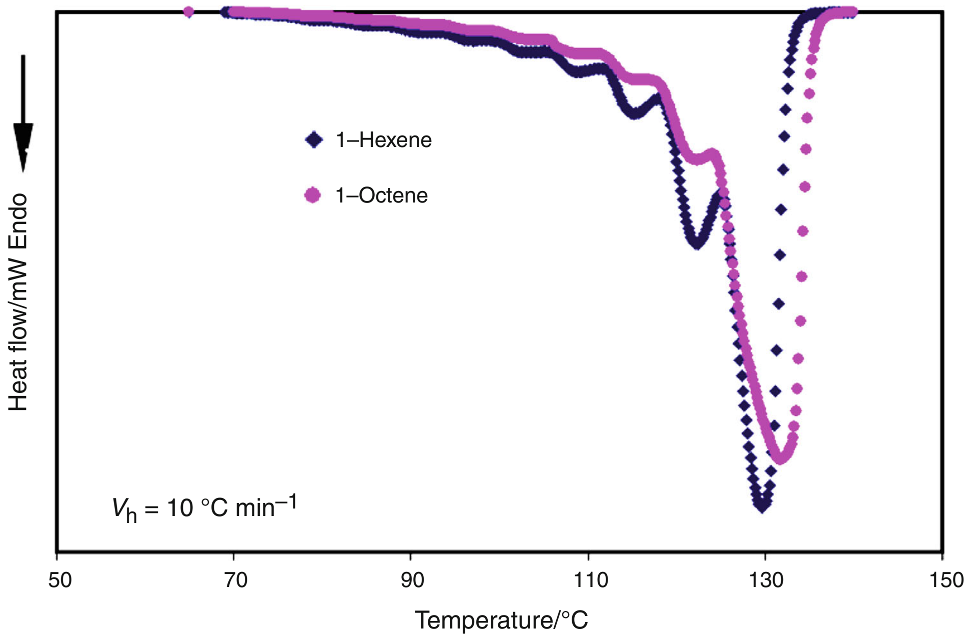

Fig. 5 Comparison of the *melting curves* of ethylene/octene and hexene (106 mmol L^{-1}) copolymers using (Ind)ZrCl$_2$/MCM-41 catalyst and the SSA method

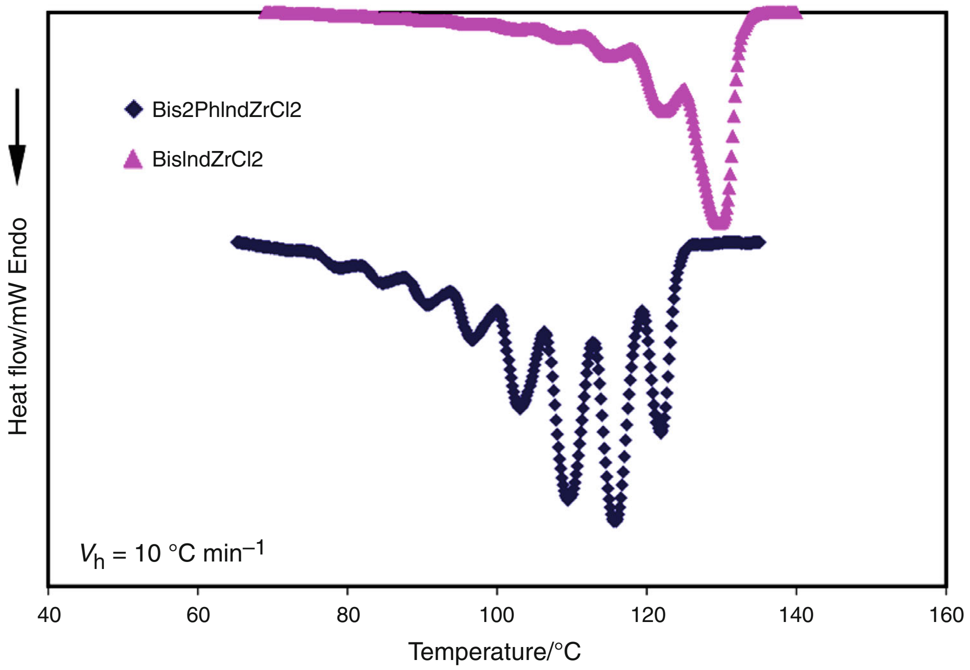

Fig. 6 Comparison of the *melting curves* of ethylene/1-hexene (106 mmol L^{-1}) copolymers obtained using (Ind)$_2$ZrCl$_2$/MCM-41 and (2-PhInd)$_2$ZrCl$_2$/MCM-41 catalysts via the SSA method

(DSCI) is very often used [31, 51, 54]. Similar DSCI values close to one are indicative of relatively homogeneous incorporation of the comonomer in the polymer chain. The thickness of different lamellae can be calculated from the Thomson–Gibbs' equation [55]:

$$T_m = T_m{}^{\circ}\,(1 - 2\delta_e/\Delta H \times l_c), \qquad (1)$$

where T_m is the observed melting point (K), $T_m{}^{\circ}$ is the equilibrium melting point of an infinite polyethylene crystal (414.5 K), δ_e is the surface energy of a polyethylene crystal ($70 \times 10e^{-3}$ J m^{-2}), ΔH is the enthalpy of fusion of 100 % crystalline polyethylene per unit volume ($288 \times 10e^{6}$ J m^{-3}), and l_c (m) is the thickness of the lamellae with melting point T_m. Mass average, l_m, and number average, l_n, lamellae thickness are defined as [56]:

$$L_m = \sum m_i l_i, \qquad (2)$$

$$l_n = 1/\left(\sum m_i/l_i\right), \qquad (3)$$

$$\text{Polydispersity} = l_m/l_n, \qquad (4)$$

where m_i is the mass fraction of lamella with thickness of l_i.

The results of lamellae thickness distribution and DSCI Values for the ethylene copolymers that were produced by two kind of indenyl-based metallocene catalysts are listed in Tables 3–7. The results show that the lamellae thickness distribution of ethylene/1-hexene copolymers was more narrow than ethylene 1-octene ones. Table 7 denotes that the $(Ind)_2ZrCl_2$ synthesized copolymers possess broader distribution of lamellae thickness than the $(2\text{-}PhInd)_2ZrCl_2$ synthesized samples. These results confirm the pervious results [31] that showed $(2\text{-}PhInd)_2ZrCl_2$ has a magnificent ability in comonomer incorporation and the supporting procedure do not affect its comonomer incorporation ability.

Moreover it was clearly observed that 1-octene resulted in more heterogeneous ethylene copolymers than 1-hexene. This behavior may be attributed to higher reactivity ratio of 1-hexene relative to 1-octene and low steric interference of 1-hexene [57]. Doubtless type and quantity of comonomer and type of catalyst have direct influence of distribution of lamellae thickness distribution.

The fractionated DSC endotherms for copolymers are shown in Fig. 4a, b. It can be seen that by increasing the comonomer content the heterogeneity of CCD decreased. Furthermore it was observed that 1-hexene copolymers have more homogeneous CCD rather than 1-octene copolymers (Fig. 5). In addition, Fig. 6 shows that the CCD of copolymers synthesized using $(2\text{-}PhInd)_2ZrCl_2$ is more homogeneous than the copolymer synthesized using $(Ind)_2ZrCl_2$.

Conclusions

$(2\text{-}RInd)_2ZrCl_2$ catalysts were supported on MCM-41 through in situ method and copolymerization performance of them was investigated. The following conclusions were obtained from the kinetic and microstructure study.

The comonomer effect factor (CEF) was decreased by increasing comonomer content and comonomer molar mass to lower value than one. The decay indexes (DI) of supported catalysts were near to one and showed the kinetic stability of the copolymerization. Addition of comonomers 1-hexene and 1-octene, decreased polymerization activity, crystallinity, density, molecular mass, and the melting point of the obtained copolymers. These behaviors were related to branching of the polymer chain. The higher the concentration of the comonomers, the lower the lamellar thickness and the smaller the crystalline length obtained. The lower value of CEF indicated that a negative comonomer effect was prevailing in copolymerization.

It was noticed that 1-hexene produced narrower lamellae thickness distribution ethylene copolymer than 1-octene and ethylene/1-octene copolymers have more heterogeneity than 1-hexene/ethylene copolymer. By increasing the comonomer content and decreasing of comonomer molar mass the heterogeneity of CCD decreased.

These results show 2-phenyl substituent in indenyl-based metallocene catalyst improve comonomer incorporation and the supporting procedure did not affect this behavior.

Acknowledgements The authors would like to thank the National Iranian Petrochemical Company-Research and Technology (NIPC-RT) for the financial support of this work, Bandar Emam Petrochemical Company (BIPC) for the GPC measurement and Japan Advanced Institute of Science and Technology (JAIST) for NMR and TREF measurement. The authors are thanks full to Prof. Terano and Dr. Taniike for the help rendered during experiments.

References

1. Heurtefeu B, Bouilhac C, Cloutet E, Taton D, Deffieux A, Cramail H. Polymer support of “single-site” catalysts for heterogeneous olefin polymerization. Prog Polym Sci. 2011;36:89–126.
2. Wannaborworn M, Praserthdam P, Jongsomgit B. Observation of different catalytic activity of various 1-olefins during ethylene/1-olefin copolymerization with homogeneous metallocene catalysts. Molecules. 2011;16:373–83.
3. Ciardelli F, Altomare A, Michelotti M. From homogeneous to supported metallocene catalysts. Catal Today. 1998;41:149–57.
4. Chakravarti S, Ray WH. Kinetic study of olefin polymerization with a supported metallocene catalyst. II. Ethylene/1-hexene copolymerization in gas phase. J Appl Polym Sci. 2001;80:1096–119.
5. Guijada R, Retuert J, Guevara JL, Rojas R, Valle M, Saavedra P, Palza H, Galland GB. Results coming from homogeneous and supported metallocene catalysts in the homo- and copolymerization of olefins. Macromol Symp. 2002;189:111–25.
6. Chu KJ, Shan CLP, Soares JBP, Penlidis A. Copolymerization of ethylene and 1-hexene with in situ supported $Et[Ind]_2ZrCl_2$. Macromol Chem Phys. 1999;200:2372–6.
7. Charles R, Estrada AN, Lugo L, Revilla J, Garcia M, Perez G. Heterogeneous copolymerization of ethylene and α-olefins using aluminohydride–zirconocene/SiO_2/MAO by high-throughput screening. Macromol Symp. 2009;285:90–100.
8. Kumkaew P, Wu L, Praserthdam P, Wanke SE. Rates and product properties of polyethylene produced by copolymerization of 1-hexene and ethylene in the gas phase with $(n\text{-}BuCp)_2ZrCl_2$ on supports with different pore sizes. Polymer. 2003;44:4791–803.
9. Hong H, Zhang Z, Chung TCM, Lee RWJ. Synthesis of new 1-decene-based LLDPE resins and comparison with the corresponding 1-octene- and 1-hexene-based LLDPE resins. Polym Sci A Polym Chem. 2007;45:639–49.
10. Choi Y, Soares JBP. Supported hybrid early and late transition metal catalysts for the synthesis of polyethylene with tailored molecular weight and chemical composition distributions. Polymer. 2010;51:4713–25.
11. Chaichana E, Khaubunsongserm S, Praserthdam P, Jongsomjit B. Effect of Ga modification on different pore size silicas in synthesis of LLDPE by copolymerization of ethylene and 1-hexene with $[t\text{-}BuNSiMe_2\ Flu]TiMe_2$/MMAO catalyst. Polym Bull. 2011;66:1301–12.
12. Carrero A, Grieken R, Paredes B. Hybrid zeolitic-mesostructured materials as supports of metallocene polymerization catalysts. Catal Today. 2012;179:115–22.

13. Grieken RV, Carrero A, Suarez I, Paraedes B. Ethylene polymerization over supported MAO/$(nBuCp)_2ZrCl_2$ catalysts: influence of support properties. Eur Polym J. 2007;43:1267–77.
14. Smit M, Zheng X, Loos J, Chadwick JC, Koning CE. Effects of methylaluminoxane immobilization on silica on the performance of zirconocene catalysts in propylene polymerization. J Polym Sci A. 2005;43:2734–48.
15. Reddy CS, Ratna D, Das CK. Polyethylene nanocomposites by gas-phase polymerization of ethylene in the presence of a nanosilica-supported zirconocene catalyst system. Polym Int. 2008;57:282–91.
16. Guo CY, Xu H, Zhang M, Yang HJ, Yan F, Yuan G. Copolymerization of ethylene and in situ-generated α-olefins to high-performance linear low-density polyethylene with a two-catalyst system supported on mesoporous molecular sieves. Polym Int. 2010;59:725–32.
17. Yan FW, Xu H, Guo GY, Zhang MG, Zhang XH, Yang HJ. Catalysis of ethylene to linear low-density polyethylene with iron-based diimine complex immobilized on calcosilicate and silica-supported rac-Et$(Ind)_2ZrCl_2$. J Appl Polym Sci. 2009;112:2298–304.
18. Guo GY, Ke Y, Liu Y, Mi X, Zhang M, Hu Y. Preparation and properties of polyethylene/montmorillonite nanocomposites formed via ethylene copolymerization. Polym Int. 2009;58:1319–25.
19. Li KT, Dai CL, Kuo CW. Ethylene polymerization over a nanosized silica supported Cp_2ZrCl_2/MAO catalyst. Catal Commun. 2007;8:1209–13.
20. De Freitas AJD, Dos Santos JHZ, Meneghetti SMP, Meneghetti MR. Polymerization of ethylene: some aspects of metallocene catalyst stabilization under homogeneous and heterogeneous reaction conditions. J Appl Polym Sci. 2011;119:3051–7.
21. Hammawa H, Wanke SE. Influence of support friability and concentration of α-olefins on gas-phase ethylene polymerization over polymer-supported metallocene/methylaluminoxane catalysts. J Appl Polym Sci. 2007;104:514–27.
22. Kumkaew P, Wanke SE, Praserthdam P, Damumah C, Kaliaguine S. Gas-phase ethylene polymerization using zirconocene supported on mesoporous molecular sieves. J Appl Polym Sci. 2003;87:1161–77.
23. Andres JA, Suarez I, Benavente R, Preze E. Characterization and properties of ethylene-propylene copolymers synthesized with homogeneous and supported metallocene catalyst in the whole range of compositions. Macromol Res. 2011;19:351–63.
24. Taniike T, Takahashi S, Wada T, Kouzai I, Terano M. Role of dispersion state of ti species in deactivation of $MgCl_2$-supported Ziegler–Natta catalysts. Macromol Res. 2010;18:839–44.
25. Randall JCJ. A review of high resolution liquid carbon nuclear magnetic resonance characterizations of ethylene-based polymers. Macromol Sci Rev Macromol Chem Phys. 1989;C29:201–317.
26. Losio S, Boccia AC, Boggioni L, Sacchi C, Ferro DR. Ethene/4-methyl-1-pentene copolymers by metallocene-based catalysts: exhaustive microstructural characterization by ^{13}CNMR spectroscopy. Macromolecules. 2009;42:6964–71.
27. Losio S, Forlini F, Boccia AC, Sacchi MC. Propene/4-methyl-1-pentene copolymers by metallocene based catalysts: first insight in ^{13}C NMR assignment. Macromolecules. 2011;44:3276–86.
28. Suarez I, Caballero MJ, Coto B. Characterization of ethylene/propylene copolymers by means of a GPC-4D technique. Eur Polym J. 2011;47:171–8.
29. Zhai YM, Wang Y, Yang W, Xie BH, Yang MB. A thermal method for quantitatively determinating the content of short chain branching in ethylene/α-olefin copolymers. J Therm Anal Calorim. 2012;110:1389–94.
30. Matsko MA, Vanina MP, Echevskaya LG, Zakharov VA. Study of the compositional heterogeneity of ethylene–hexene-1 copolymers by thermal fractionation technique by means of differential scanning calorimetry. J Therm Anal Calorim. 2013;113:923–32.
31. Mortazavi SMM, Arabi H, Zohuri GH, Ahmadjo S, Nekoomanesh M, Ahmadi M. Copolymerization of ethylene/α-olefins using bis(2-phenylindenyl)zirconium dichloride metallocene catalyst: structural study of comonomer distribution. Polym Int. 2010;59:1258–65.
32. Nekoomanesh M, Arabi H, Nejabat GR, Emami M, Zohuri GH. Preparation of polyethylene nano-fibres using rod-like MCM-41/$TiCl_4$/$MgCl_2$/THF Bi-supported Ziegler–Natta catalytic system. Iran J Polym Sci Technol. 2008;3:243–50.
33. Mortazavi SMM, Arabi H, Zohuri GH, Ahmadjo S, Nekoomanesh M, Ahmadi M. Ethylene homo- and copolymerization using a bis-$IndZrCl_2$ metallocene catalyst: structural composition distribution of the copolymer. Macromol React Eng. 2009;3:263–70.
34. Awudza JAM, Tait PJT. The "comonomer effect" in ethylene/α-olefin copolymerization using homogeneous and silica-supported Cp_2ZrCl_2/MAO catalyst systems: some insights from the kinetics of polymerization, active center studies, and polymerization temperature. J Polym Sci A Polym Chem. 2008;46:267–77.
35. Bchoteco E, Vecino M, Montes M, Lacal JC. Kinetics and properties in metallocene catalysed propene polymerizations. Chem Eng Sci. 2001;56:4169–79.
36. Marques MFV, Marinna A. Zeolite-supported metallocene catalyst for ethylene/1-hexene copolymerization. J Polym Sci A Polym Chem. 2004;42:3038–48.
37. Kumkaew P, Wu L, Praserthdam P, Wanke SE. Rates and product properties of polyethylene produced by copolymerization of 1-hexene and ethylene in the gas phase with $(n\text{-}BuCp)_2ZrCl_2$ on supports with different pore sizes. Polymer. 2003;44:479–4803.
38. Uozumi T, Toneri T, Soga K. Copolymerization of ethylene and 1-octene with $Cp^{*}TiCl_3$ as catalyst supported on 3-aminopropyltrimethoxysilane treated SiO_2. Macromol Rapid Commun. 1997;18:9–15.
39. Czaja K, Bialek M, Utrata A. Copolymerization of ethylene with 1-hexene over metallocene catalyst supported on complex of magnesium chloride with tetrahydrofuran. J Polym Sci Polym Chem. 2004;42:2512–9.
40. Al-Malaika S, Peng X, Watson H. Metallocene ethylene-1-octene copolymers: influence of comonomer content on thermo-mechanical, rheological, and thermo-oxidative behaviours before and after melt processing in an internal mixer. Polym Degrad Stab. 2006;91:3131–48.
41. Hosoda S, Hori H, Yada KI, Nakahara S, Tsuji M. Degree of comonomer inclusion into lamella crystal for propylene/olefin copolymers. Polymer. 2002;43:7451–60.
42. Grieken R, Carrero A, Suarez I, Paredes B. Effect of 1-hexene comonomer on polyethylene particle growth and kinetic profiles. Macromol Symp. 2007;259:243–52.
43. Kim I, Kim KT, Lee MH, Do Y, Chung H. Copolymerization of ethylene and 1-decene by metallocenes: direct comparison of $Me_2C(Cp)(Flu)ZrMe_2$ with $Et(Cp)(Flu)ZrMe_2$. Polym Eng Sci. 2001;41:899–907.
44. Cong R, DeGroot W, Parrott A, Yau W, Hazlitt L, Brown R, Miller M, Zhou ZH. New technique for characterizing comonomer distribution in polyolefins: high-temperature thermal gradient interaction chromatography (HT-TGIC). Macromolecules. 2011;4:3062–72.
45. Miller MD, DeGroot AW, Lyons JW, Damme FAV, Winniford BL. Separation of polyolefins based on comonomer content using high-temperature gradient adsorption liquid chromatography with a graphitic carbon column. J Appl Polym Sci. 2012;123:1238–44.
46. Wild L. Temperature rising elution fractionation. Adv Polym Sci. 1991;98:1–47.
47. Neves CJ, Monteiro E, Habert AC. Characterization of fractionated LLDPE by DSC, FTIR, and SEC. J Appl Polym Sci. 1995;50:817–24.
48. Zhou X, Hay JN. Fractionation and structural properties of linear low density polyethylene. Eur Polym J. 1993;29:291–300.

49. Feng Y, Jin X. Fractionation and characterization of a LLDPE synthesized by a metallocene catalyst. Polym Plast Technol Eng. 1998;37:271–83.
50. Anantawaraskul S, Soares JBP, Wood-Adams PM, Monrabal B. Effect of molecular weight and average comonomer content on the crystallization analysis fractionation (Crystaf) of ethylene α-olefin copolymers. Polymer. 2003;44:2393–401.
51. Bialek M, Czaja K, Majewska BS. Studies of structural composition distribution heterogeneity in ethylene/1-hexene copolymers using thermal fractionation technique (SSA): effect of catalyst structure. Thermochim Acta. 2005;429:149–54.
52. de Gáscue BR, Prin JL, Hernández G, Vallés EM, Lorenzo AT, Müller AJ. Use of the successive self-nucleation and annealing technique to characterize 60 Co gamma irradiated HDPEs. J Therm Anal Calorim. 2011;103(2):669–78.
53. Chen YP, Fan ZH. Ethylene/1-hexene copolymerization with $TiCl_4/MgCl_2/AlCl_3$ catalyst in the presence of hydrogen. Eur Polym J. 2006;42:2441–9.
54. Starck P, Lofgren B. Thermal properties of ethylene/long chain α-olefin copolymers produced by metallocenes. Eur Polym J. 2002;38:97–107.
55. Hosoda S. Structural distribution of linear low-density polyethylenes. Polym J. 1998;20:383–97.
56. Razavi-Nouri M. Studies of comonomer distributions and molecular segregations in metallocene-prepared polyethylenes by DSC. Polym Test. 2006;25:1052–8.
57. Paredes B, Grieken R, Carrero A, Suarez I, Soares JBP. Ethylene/1-hexene copolymers produced with $MAO/(nBuCp)_2ZrCl_2$ supported on SBA-15 materials with different pore sizes. Macromol Chem Phys. 2011;212:1590–9.